

Lasers in caries diagnosis and prevention

Denise M. Zezell^{a,*}, Patricia A. da Ana^a, Adriana C. Ribeiro^{a,b}, Luciano Bachmann^{a,c},
Anderson Z. Freitas^a and Nilson Dias Vieira Jr^a

^a*Instituto de Pesquisas Energéticas Nucleares, IPEN/CNEN-SP, USP, São Paulo, Brazil*

^b*Departamento de Endodontia, Faculdade de Odontologia, USP, São Paulo, Brazil*

^c*Faculdade de Filosofia Ciências e Letras, USP, Ribeirão Preto, Brazil*

Abstract. This study evaluated the potential of Erbium laser in caries prevention and optical methods for diagnosis. Temperature rise was measured by an infrared thermographic camera. Chemical and structural changes were identified by FTIR. Natural and artificial lesions were examined by optical coherence tomography. Laser irradiation resulted in a surface temperature rises around 400°C, loss of water, change of the collagen and increase of the OH⁻ radical and a small change in the mineral matrix. OCT analysis produced a dentin-enamel tomogram with 10 μm resolution. Fluorescence spectroscopy and OCT system were able to detect and differentiate early caries in its structure.

Keywords: Caries diagnosis, caries prevention, FTIR, optical coherence tomography

1. Introduction

1.1. Lasers for caries prevention

Highly absorbed wavelengths can modify the tissue composition and structure by thermal action, and promote an increased acid resistance [4]. One of the most absorbed laser wavelength by the enamel are Erbium wavelengths (2.94 μm @ Er:YAG and 2.79 μm @ Er,Cr:YSGG), for which the primary absorption occurs for water and hydroxiapatite. The Er,Cr:YSGG has a slight advantage over Er:YAG because it faces greater absorption by the hydroxiapatite, which results in higher surface temperature.

The absorption of laser energy by specific components of dental enamel is converted directly into heat; this thermal effect is regarded as being the cause of microstructural and chemical changes and serves to explain the increase in acid resistance. Currently it is widely accepted that bound carbonate is released when dental enamel is heated. Therefore, it is important to know the right temperatures related to several laser fluences in order to choose the appropriate laser condition and to assure the reduction of acid solubility without pulpal damage.

Besides that, chemical composition changes must be monitored for each laser fluence.

*Corresponding author. Tel.: +55 11 3816 9313; Fax: +55 11 3816 9315; E-mail: zezell@usp.br

1.2. Lasers for caries detection

The caries diagnosis is achieved by low absorbed wavelengths that penetrate deeply in the tissue and make possible the analysis of the caries lesions at sub-superficial layers that could not be visualized by conventional methods. The optical coherence tomography (OCT) is the first diagnostic imaging technology in which coherent optics features are important. OCT is a novel imaging technology that produces high-resolution cross-sectional images of the internal microstructure of living tissue [7]. The optical sectioning ability of OCT is achieved by exploiting the short temporal coherence of a broadband light source. The OCT scanners enables visualize the microscopic structures in tissue at depths layers.

2. Materials and methods

2.1. Temperature rise

Twenty-four bovine teeth were selected, cleaned and sectioned at a bucco-lingual plane with a diamond saw disk. Teeth were randomly divided into four groups, according to the laser fluences and the presence of a photoabsorber: G1 – 2.8 J/cm² with photoabsorber; G2 – 2.8 J/cm² without photoabsorber; G3 – 8.5 J/cm² with photoabsorber; G4 – 8.5 J/cm² without photoabsorber. It was used an Er,Cr:YSGG laser, which has 2.79 μm wavelength, 140–200 μs of temporal width and 20 Hz of repetition rate. The laser is coupled to a fiber optics delivery system with 430 μm of spot size, with 600 μm diameter. In all samples, laser irradiation was performed without air/water mist.

A thin layer of coal paste ($\sim 100 \mu\text{m}$) diluted in equal parts of deionized water and 99% ethanol was applied over the buccal surface to absorb laser energy. The temperature changes in enamel surface during and immediately after laser irradiation were measured using a thermographic camera (ThermaCam FLIR SC3000 Systems, USA), which stores infrared images and data at rates up to 900 Hz. This experiment was performed at a room temperature of 25°C, 47% air relative humidity and considering emissivity of teeth 0.91.

2.2. Chemical composition

The samples used in infrared spectroscopy were bovine incisors; which were stored in sodium chloride solution at 0.9 wt.% until sample preparation. The samples were cut to produce a block of tissues, and they were sanded to produce flat surfaces. The sample irradiation was performed with an Er:YAG laser, with emission at 2.94 μm (3401 cm^{-1}), pulse width of 400 μs , and repetition rate of 2 Hz. To irradiate the entire sample area (diameter $\sim 2 \text{ mm}$) 1 up to 20 pulses (approximately) were applied onto the surface. The spectral acquisition was alternated with the sample irradiation – first the spectrum of the non-irradiated sample was acquired, then sequentially the irradiation was applied to the sample, from the least fluency successively up to the higher value (4.3 J/cm²).

Fourier transform infrared spectrometer (Magna-IR System 850 series II, Nicolet, Madison, United States of America) was used. The spectral region analyzed was between 4000 cm^{-1} and 400 cm^{-1} (2.5 μm and 25 μm) at the reflection mode, and a sample holder with specific diameter holes was used in order to select the region in the irradiated sample.

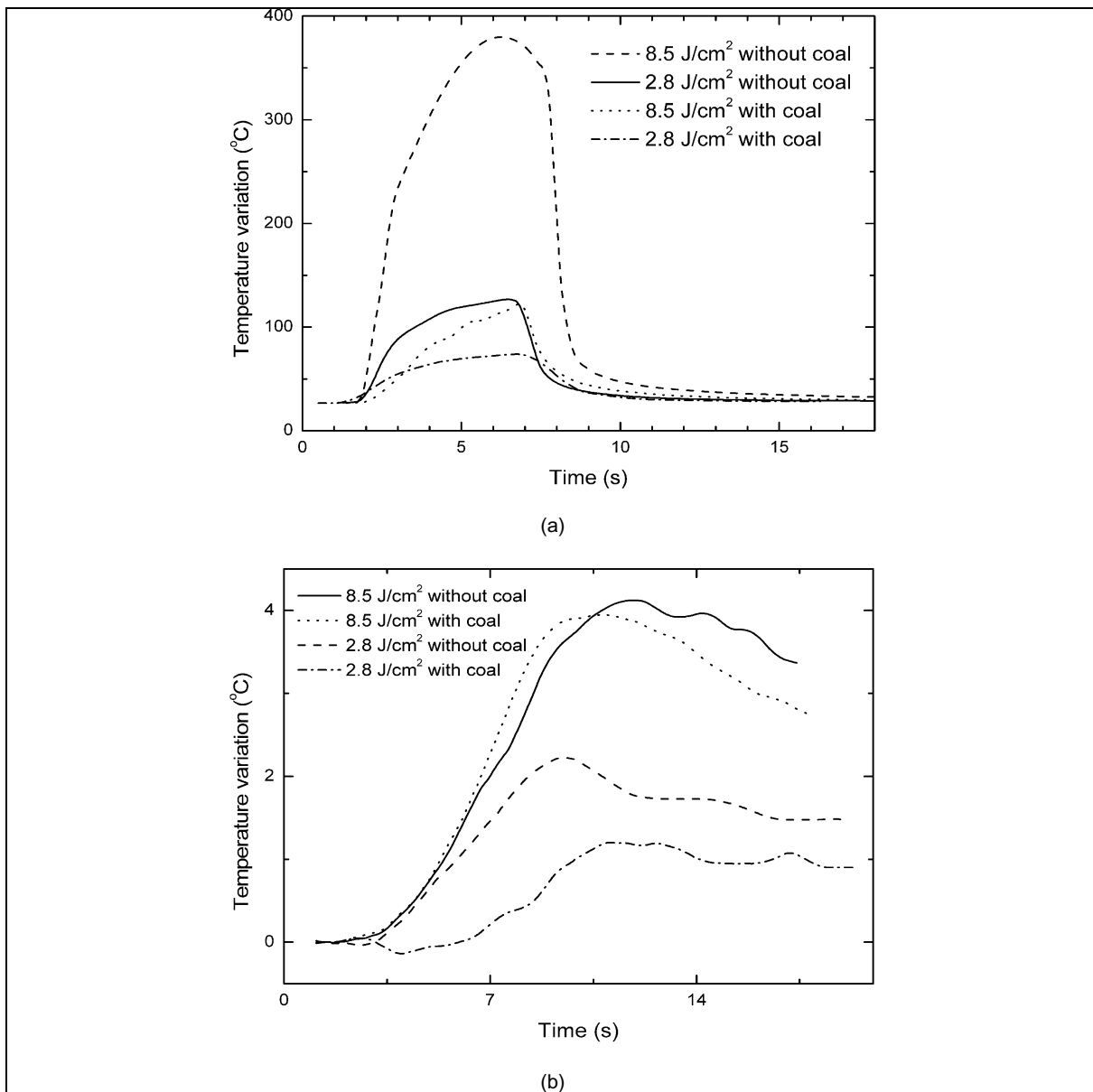


Fig. 1. Curves of reached temperature during Er,Cr:YSGG laser irradiation in a standardized point located at the enamel surface (a) and at dentin-pulp limit (b).

2.3. Caries detection

Artificial caries lesions were produced in five human teeth by the pH demineralization and remineralization cycling model, as performed by Featherstone et al. [5].

The configuration employed in OCT system was the open air Michelson interferometer type. The system utilized a Ti:Al₂O₃ laser operating in the mode-locking regime femto-second laser source (Mira-Coherent) centered around 830 nm with a 50 fs pulse width and 40 nm FWHM spectral width which

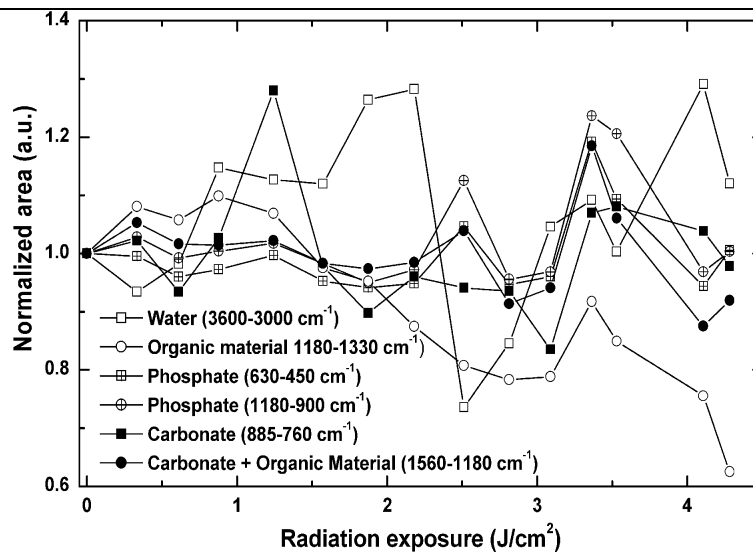


Fig. 2. Normalized area of infrared absorption bands of irradiated enamel with radiation exposure below 4.2 J/cm^2 . Each data was normalized by the area of the natural sample area.

Almost all observed bands keep constant after irradiation up to the highest exposure radiation.

provided 100 mW of optical power. The delay line was implemented with a scanner operating at a frequency of 200 Hz, a grating of 590 grooves/mm with $25 \times 25 \text{ mm}$ of dimension, and a lens with 50 mm of focal length. It was used a low noise amplifier and a detector coupled to a digital oscilloscope to store the data (Tektronix 3000B) and save them in the computer. The laser beam was focused into the teeth with a lens of 50 mm of focal length, providing a lateral resolution of $10 \mu\text{m}$. The image was produced with a lateral and axial scans step of $10 \mu\text{m}$. The maximum depth was 3 mm.

3. Results and discussion

3.1. Temperature rise

The temperature variation was registered at the enamel and at pulp-dentin limit. The maximum surface temperature peaks were 420°C and 132°C in the samples irradiated with 8.5 J/cm^2 without and with coal paste, respectively. For samples irradiated with 2.8 J/cm^2 without and with coal paste the maximum temperature rise was 130°C and 80°C . These temperature increases which agrees with the findings reported by Fried et al. [6]. After the end of irradiation, the temperatures fitted to an exponential decay, reaching nearly its initial temperature value. In all samples irradiated without the coal paste, surface temperature was higher than in samples irradiated with the coal paste. The average rise recorded by thermographic camera at enamel surface was 75.6°C and 126°C in groups G1 and G3, respectively in recovered samples and 126.5°C and 350°C in groups G2 and G4, respectively. The maximum surface temperature peaks probably were higher considering the reported melting produced in samples irradiated with the same energy, which implies in temperature ranges near of melting of hydroxiapatite (about 1200°C) [2]. In fact, the scanning speed of the thermocamera seems to be unable to detect the peak instantaneous temperatures achieved from the $200 \mu\text{s}$ pulses of the Er,Cr:YSGG laser.

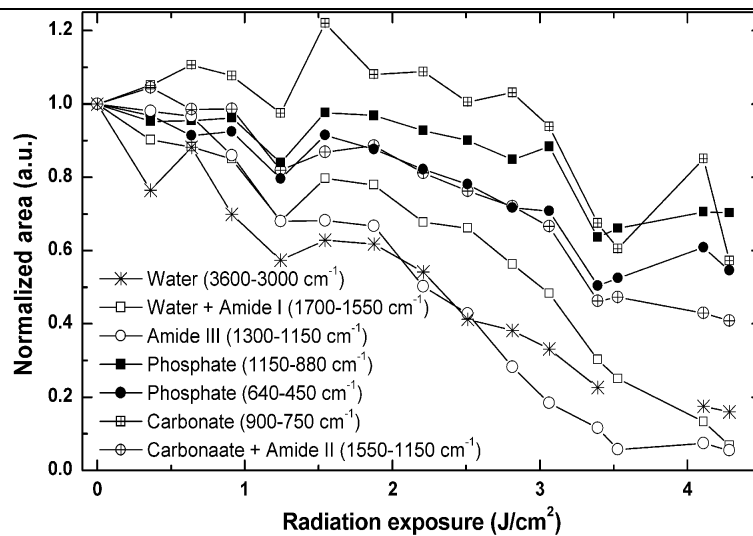


Fig. 3. Normalized area of infrared absorption bands of irradiated dentin with radiation exposure below 4.2 J/cm^2 . Each data was normalized by the area of the natural sample area. We observe a major reduction of water and organic material while the inorganic radicals show only a little decrease.

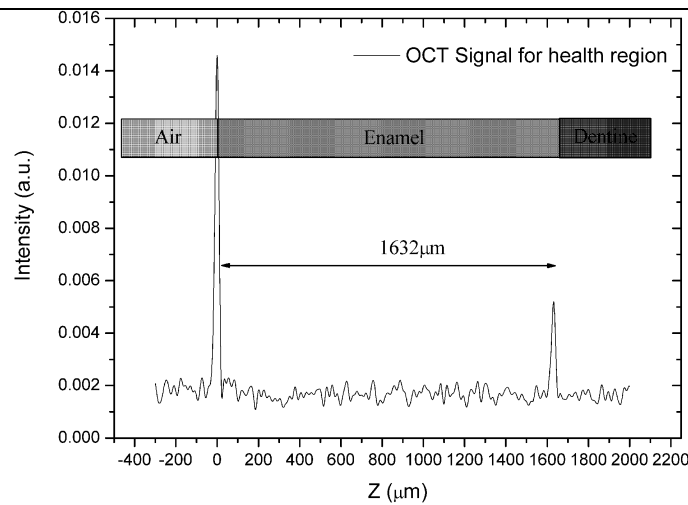
The application of a photoabsorber before laser irradiation aimed to increase the absorption of the laser beam at the enamel surface, which could guarantee that the heat produced due to laser absorption in the coating material is transmitted into the adjacent enamel. This procedure avoids the excessive laser beam penetration in deeper dental structures and decreases the risk of damages in dental pulp [3,8].

The maximum dentin temperature variations were 4°C in all samples irradiated with 8.5 J/cm^2 (with and without coal). In samples irradiated with 2.8 J/cm^2 , the maximum variations were 1.2°C and 2.2°C with and without coal, respectively. The dentin temperatures did not exceed the critical threshold of 5.6°C reported to be dangerous to pulp vitality [9]. When irradiation was stopped, the surface temperature decreased immediately, which did not happen with the pulpal temperature that needed more than 30 s to get back to its baseline.

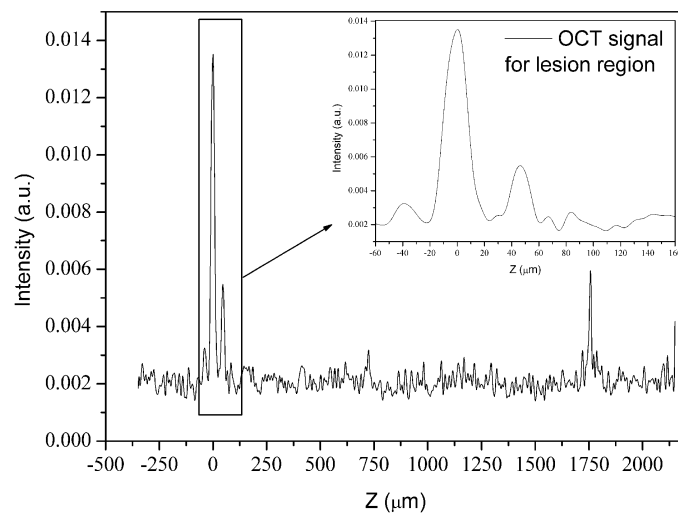
3.2. Chemical composition

The inorganic matrix of irradiated enamel and dentin was monitored by band area of the phosphate radicals: 1094 cm^{-1} , 1044 cm^{-1} , 955 cm^{-1} , 603 cm^{-1} and 570 cm^{-1} ; carbonate radicals: 1534 cm^{-1} , 1442 cm^{-1} , 1395 cm^{-1} and 866 cm^{-1} . The water was monitored by the band between $3600\text{--}3000 \text{ cm}^{-1}$, while the organic matrix was monitored by the bands between 1180 cm^{-1} e 1320 cm^{-1} . After irradiation with the highest fluence only the organic material shows a little decrease while the other inorganic radicals and water keeps constant. The water and organic matrix bands in dentin are a little higher than in enamel; and the water was monitored by the bands positioned at: $3000\text{--}3500 \text{ cm}^{-1}$ and $1700\text{--}1550 \text{ cm}^{-1}$; and the organic matrix by the bands at: $1300\text{--}1150 \text{ cm}^{-1}$ (amide III collagen structure), $1600\text{--}1300 \text{ cm}^{-1}$ (amide II) and $1700\text{--}1550 \text{ cm}^{-1}$ (amide I).

At enamel samples, all inorganic radicals are roughly constant up the irradiation with 4.2 J/cm^2 and only the organic material shows a little decrease after irradiation. Despite the water is thermally unstable, this molecule has low concentration in enamel, and does not decrease with the irradiation. At the irradiated dentin, the amide III, amide I and water show the higher decrease after laser irradiation



(a)



(b)

Fig. 4. OCT signal from tooth health region (a) and detail of OCT signal from tooth lesion region (b). The second peak is the back surface of the lesion. The upper right corner is the total scan.

while the other inorganic radicals decrease also but not so fast as the organic material. The decrease of all inorganic bands at increasing radiation exposure is assigned to increasing of infrared signal scattering by the surface. The infrared spectroscopy determines effectively the chemical changes due to laser irradiation.

3.3. Caries detection

In Fig. 4(a) can be seen two main peaks, which separates the region into three parts. The first one, in light gray, corresponds to the air; the gray corresponds to enamel and the region in dark gray color corresponds to dentine. The OCT signal of the region where the lesion was located shows a different

behavior in relation to the healthy region. The first peak presents a second structure corresponding to the back surface of the lesion region. The distance between the first peak, which corresponds to the air/enamel interface, and the second one, which corresponds to the enamel/lesion interface, depends on the structure of the lesion. In Fig. 4 (b), this distance was 40 μm .

With this system, it was possible to depict internal structures of teeth and to detect early caries lesions. In this study, it was not possible to measure the reflectivity variation like was performed by other authors [1]. Nevertheless, with the improvement of the system, it will be possible to generate images in real time. In the future, the OCT system will provide a powerful contactless diagnostic method that could replace the X-ray radiography, with the convenience of no hazard ionization radiation. Therefore, the OCT system has shown to be a prospective method for caries diagnosis, but more researches are still necessary to guarantee the improvement of this system and its clinical applicability.

Acknowledgements

To PROCAD-CAPES, CNPq, British Council and FAPESP for giving support for this investigation.

References

- [1] B.T. Amaech, A.G. Podoleanu, G.N. Komarov, J.A. Rogers, S.M. Higham and D.A. Jackson, Application of optical coherence tomography for imaging and assessment of early dental caries lesions, *Laser Physics* **13** (2003), 703.
- [2] L. Bachmann, A.F. Craievich and D.M. Zezell, Crystalline structure of dental enamel after Ho:YLF laser irradiation, *Arch Oral Biol* **49** (2004), 923–929.
- [3] H.G.D. Boari, D.M. Zezell and C.P. Eduardo, Dye-enhancing Nd:YAG irradiation of enamel aiming caries prevention, *J Dent Res* **79** (2000), 1079–1079.
- [4] J.D.B. Featherstone, D. Fried and E. Bitten, Mechanism of laser induced solubility reduction of dental enamel, *SPIE* **2973** (1997), 112–116.
- [5] J.D.B. Featherstone, M.M. O'Reilly, M. Shariati et al., Enhancement of remineralization *in vitro* and *in vivo*, in: *Factors Relating to Demineralization and Remineralization of the Teeth*, S.A. Leach, eds, Oxford, IRL Press, 1986, pp. 23–34.
- [6] D. Fried, J.D.B. Featherstone, S.R. Visuri, W. Seka and J.T. Walsh, The caries inhibition potential of Er:YAG and Er:YSGG laser radiation, *SPIE* **2672** (1996), 37–78.
- [7] D. Huang, E.A. Swanson, C.P. Lin, J.S. Schuman, W.G. Stinson, W. Chang, M.R. Hee, T. Flotte, K. Gregory, C.A. Puliafito and J.G. Fujimoto, Optical coherence tomography, *Science* **254** (1991), 1178–1181.
- [8] T. Morioka, K. Suzuki and S. Tagomori, Effect of beam absorptive mediators on an acid-resistance of surface enamel by Nd:YAG laser irradiation, *J Dent Health* **34** (1984), 40–44.
- [9] L. Zach and G. Cohen, Pulp response to externally applied heat, *Oral Surg* **19** (1965), 515–530.